EUROfusion

WPMAT-PR(18) 21323

M. Dias et al.

New WC-Cu composites for the divertor in fusion reactors

Preprint of Paper to be submitted for publication in
Journal of Nuclear Materials

This work has been carried out within the framework of the EUROfusion Consortium and has received funding from the Euratom research and training programme 2014-2018 under grant agreement No 633053. The views and opinions expressed herein do not necessarily reflect those of the European Commission.

New WC-Cu composites for the divertor in fusion reactors

M. Dias [1], N. Pinhão [1], R. Faustino [1], R.M.S. Martins [1], A. S. Ramos [2], M. T. Vieira [2], J.B. Correia [3], E. Camacho[4], F.M. Braz Fernandes[4], B. Nunes[5,6], A. Almeida[5], U.V. Mardolcar [7], E. Alves [1]

[1] Instituto de Plasmas e Fusão Nuclear, Instituto Superior Técnico, Universidade de Lisboa, Av. Rovisco Pais, 1049-001, Lisboa, Portugal

[2] CEMMPRE, Department of Mechanical Engineering, University of Coimbra, R. Luís Reis Santos, 3030-788 Coimbra, Portugal;

[3] LNEG, Laboratório Nacional de Energia e Geologia, Estrada do Paço do Lumiar, 1649-038 Lisboa, Portugal

[4] CENIMAT/I3N, Departamento de Ciência dos Materiais, Faculdade de Ciências e Tecnologia, FCT, Universidade NOVA de Lisboa, Quinta da Torre, 2829-516 Caparica, Portugal

[5] CeFEMA, Center of Physics and Engineering of Advanced Materials, Instituto Superior Técnico, Universidade de Lisboa, Av. Rovisco Pais, 1049-001 Lisboa, Portugal

[5]Atlântica, Escola Universitária de Ciências Empresariais, Saúde, Tecnologia e Engenharia, Fábrica da Pólvora de Barcarena, 2730-036 Barcarena, Portugal

[7] Departamento de Física, Instituto Superior Técnico, Av. Rovisco Pais, 1049-001 Lisboa Portugal

CORRESPONDING AUTHOR:
Marta Dias

Instituto de Plasmas e Fusão Nuclear, Instituto Superior Técnico, Universidade de Lisboa, Av. Rovisco Pais, 1049-001, Lisboa, Portugal

Telephone: +351 21 9946000

Fax: +351 21 9550117

Email: marta.dias@ctn.ist.utl.pt

Abstract

The requirements for the divertor components of future fusion reactors are challenging and therefore a stimulus for the development of new materials. In this paper, WC-Cu composites are studied for use as thermal barrier between the plasma facing tungsten tiles and the copper-based heat sink of the divertor. Composite materials with 50 % vol. WC were prepared by hot pressing and characterized in terms of microstructure, density, expansion coefficient, elastic modulus, Young's modulus and thermal diffusivity. The produced materials consisted of WC particles homogeneously dispersed in a Cu matrix with densifications between 88 % and 98 %. The sample with WC particles coated with Cu evidenced the highest densification. The thermal diffusivity was significantly lower than that of pure copper or tungsten. The sample with higher densification exhibits a low value of Young's modulus (however, it is higher compared to pure copper), and an average linear thermal expansion coefficient of 13.6×10^{-6} $^{o}C^{-1}$ in a temperature range between 100 ^{o}C and 550 ^{o}C. To estimate the behavior of this composite in actual conditions, a monoblock of the divertor in extreme conditions was modelled. The results predict that while the use of WC-Cu interlayer leads to an increase of 190 ºC on the temperature of the upper part of the monoblock when compared to a pure Cu interlayer, the composite will improve and reduce significantly the cold-state stress between this interlayer and the tungsten.

Keywords: WC-Cu composite, hot pressing, thermal diffusivity, densification, modelling

1. Introduction

The heat generated in nuclear fusion reactors will be extracted by the first wall of the blanket and in the water-cooled divertor. It is intended to perform a heat collection without losses, which requires materials that can withstand intense neutron irradiation and very high heat fluxes, without compromising their physical integrity. The present design for the water-cooled divertor consists of tungsten monoblocks crossed by a CuCrZr pipe where the coolant circulates. Tungsten was chosen to be the plasma facing component due to the low sputtering [1], high melting point and a low tritium retention at high temperatures. However, the tungsten grades presently available are associated with relatively high ductile-to-brittle transition temperature and therefore show a high probability of failure at room temperature during, for instance, repair/cleaning operations after high temperature service [2]. The CuCrZr alloy is the most promising heat sink material due to its high conductivity and ductility, allied to high strength and microstructural stability [1]. The service temperature of CuCrZr, however, is relatively low and the material suffers embrittlement under irradiation [3]. Therefore, there is a thermal operation gap as well as a thermal strain mismatch between the two materials, induced by the dissimilar values of coefficient of thermal expansion (CTE) [3][4]. For these reasons a thermal barrier interlayer between the tungsten and the CuCrZr heat sink is required.

While pure copper is presently used as interlayer, several composites have been studied for this purpose. Several authors have investigated a W-Cu interlayer [5,6,7].

The critical drawback of W-Cu composite, however, is the loss of strength at elevated temperatures owing to the softening of the copper matrix [8]. Schöbel et al. [9] suggests a W-monofilament reinforced Cu composite (Wf-Cu) as a promising interlayer. The results, however, revealed that the stress mismatch in the W-wires between the matrix and the filaments lead to thermal fatigue damage during thermal cycling [10].

The present work focuses on copper matrix composites with tungsten carbide (WC) particles as reinforcing phase. WC combines favourable properties, such as high melting point [11] good wettability by molten copper [11], and, compared to W, has a higher CTE [12] and lower thermal conductivity [13] making it a good choice as reinforcing phase. Both carbon and tungsten have a very low solubility in liquid copper and the high hardness of WC [11] is expected to act as a mechanical reinforcement of the composite material. In order to understand the advantage of using the WC-Cu cermet on the divertor, the response between a monoblock with a WC-Cu cermet interlayer and with a pure copper interlayer was compared, under the effect of slow transient heat pulse (20 MW/m^2 in 10 s).

2. Experimental

WC-Cu powder mixtures with 50 v/v % WC were produced by turbula blending for 1 h in N_2 atmosphere, commercially pure WC powder with 99.9 % nominal purity with Cu powder (irregular particles with size < 37 μm) with 99.99 % nominal purity. The details of the samples produced are in table 1. All the WC-Cu powders were consolidated by hot pressing in an Idea Vulcan 70 VP press at a temperature of 1060 ºC using loads of 37 MPa with a heating rate of ~2 ºC/s on graphite dies of 10 x 55 x 5

mm^3. The thermomechanical cycle was optimized to minimize the outflow of liquid metal.

In one case (sample 3) the WC particles were previously coated with a Cu layer deposited by magnetron sputtering deposition. For this purpose, a locally made sputtering equipment was used, including a special mechanism to mix the powders with random movement ensuring that the particles' surface is uniformly exposed to the plasma. After attaining a base pressure below $5x10^{-4}$ Pa, argon was introduced in the deposition chamber up to ~$5x10^{-1}$ MPa and a power of 600 W was applied to the Cu sputtering target to start the deposition process. The selected deposition parameters resulted in the development of a nanocrystalline Cu thin film around the WC particles.

Table 1 – Samples details.

Sample	**Grain size (µm) and Conditions**	
50WC-50Cu %(v/v)	WC	Cu
Sample 1	1	37
Sample 2	18	37
Sample 3	WC with 18 µm coated with Cu	37

The microstructures of the consolidated materials were investigated using the secondary and backscattered electron signals (SE and BSE, respectively) on polished as-sintered surfaces, using a JEOL JSM-7001F scanning electron microscopy (SEM) operated at an accelerating voltage of 20 kV and coupled with energy dispersive X-ray spectroscopy (EDS).

The density of the samples was measured using the Archimedes method. Thermal diffusivity measurements were performed with a laser flash instrument Flash Line 5000 Anter Corporation in the 100– 400 ºC temperature range.

Based on the high densification results, only sample 3 (50WC-50Cu

composition, with WC particles coated with Cu layer) was used for the measurement of the thermal expansion coefficient and Young's modulus. The experimental values obtained for this sample were used for the modelling study. The thermal expansion coefficient was measured using the thermomechanical analyser Linseis TMA PT1600 with an alumina sample holder and a heating/cooling rate of 10 ^{o}C/min from room temperature to 850 ^{o}C and performed at ambient atmosphere.

The Young's modulus measurements were performed by the identation method in a Shimadzu DHU-211S ultramicroindenter, using a Berkovich indenter with an edge angle of 115°. The tests were made using a load-creep-unload cycle. The maximum load was chosen to produce in all samples an indentation depth smaller than 100 nm. In this way, after preliminary tests, the samples were indented at a constant rate of 0.35033 mN/s until a maximum load of 5 mN. The creep stage at maximum load had a duration of 20 s. The Young's modulus was determined from the analysis of the unloading section of the load-displacement curves obtained.

In order to understand the thermal behaviour of the WC-Cu cermet, a finite elements modelling (FEM) study of the temperature and stresses on the monoblock divertor target, with a standard interlayer of copper and with an interlayer of the 50WC-50Cu cermet, was performed. The geometry adopted corresponds to the specifications for the 2nd design phase of the DEMO reactor (WPDIV) with a tungsten monoblock of 28x23x12 mm^3, with a minimum vertical distance of 8 mm between the plasma facing surface and the interlayer[1]; a CuCrZr cooling tube with (OD/ID = 15/12 mm) and an interlayer of 1 mm thickness of either copper or cermet. Due to the symmetry, only one quarter of the block was modelled. Figure 1 illustrates the geometry and the mesh used.

1 Note that this represents an increase of 3 mm comparing with previous specifications. This increase implies an increase of the maximum temperature of the surface of approximately 200 °C in comparison with similar ITER results.

A rectangular transient heat flux pulse of 20 MW/m^2 for 10 s, corresponding to the maximum heat flux load expected in DEMO was applied. The effect of the coolant water is simulated considering a constant temperature of water of 130 °C and a heat transfer coefficient between the cooling tube and the water of 200 $Wm^{-2}K^{-1}$, corresponding to the high end of the values computed in [14]. The temperature dependence of material properties was considered according to [15] for tungsten, copper and the CuCrZr tube. For the 50WC-50Cu cermets the experimental results measured in this work were used and are indicated in Table 1. Thermal radiation emission was considered on the plasma facing and lateral faces.

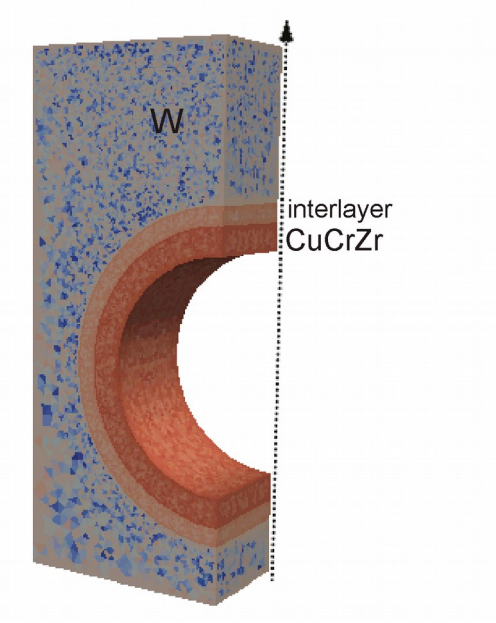

Figure 1 - Geometry and mesh used for the FEM model. The geometry corresponds to a quarter part of a monoblock. The arrow indicates the position of the vertical axis.

The stresses were computed considering a stress-free temperature of 580 ºC, corresponding to the typical joining temperature of the fabrication techniques used [16]. The Open Source packages Gmsh [17] and Elmer [18] were used, respectively for the geometry and grid computation and for the thermal and linear elasticity models.

3. Results and discussion

3.1 Materials production and characterization

Figure 2 shows the microstructures of all the three samples produced with the 50WC-50Cu composition. All consolidated materials consisted of WC particles dispersed in a Cu matrix without any evidence of oxide formation. The microstructure of sample 1, which only contains WC particles with 1μm size (Figure 2 (a) and (e)), evidences large WC aggregates with an average size of ~20 μm. These probably represent uninfiltrated agglomerates of WC powder or Cu particles loosely lumped which were incompletely wet during hot pressing.

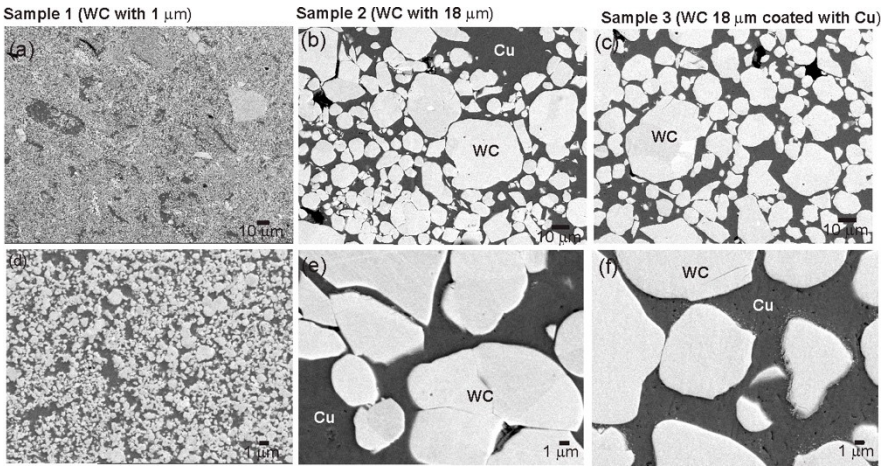

Figure 2 – SEM/BSE images showing the microstructure of 50WC-50Cu cermet with different grain sizes (a) and (d) WC with 1μm, (b) and (e) WC with 18μm, (c) and (f) WC with 18 μm particles coated with a Cu layer.

Different densifications were obtained for the materials as presented in Table 2. For samples 1 and 2 with single size WC of 1 μm and 18 μm, respectively, the densification values were similar, which suggests that, in this case, densification is not related with the WC grain size. Sample 3 (WC with 18 μm coated with Cu layer) evidences a higher densification, probably due to the strong interface between the coated

WC particles and the Cu matrix. The results indicate that in these composites and consolidation conditions (1060 ºC and 37 MPa), we were able to obtain an almost complete densification only for sample 3 (WC with 18 μm coated with Cu layer).

Table 2 – Densification values of the 50WC-50Cu samples.

Samples	Densification
Sample 1 (WC with 1μm)	88% [20]
Sample 2 (WC with 18 μm)	88%
Sample 3 (WC particles coated with Cu layer)	98%

Figure 3 presents the thermal diffusivity of two 50WC-50Cu samples (sample 1 and 3) as a function of temperature together with literature values for pure Cu [21], CuCrZr [22], W [23] and WC [24]. The thermal diffusivity behavior of both samples is between values of pure Cu and those for pure WC. However, the sample with higher WC sizes (sample 3) evidences a higher thermal diffusivity values. This effect is justified by the fact that increasing the grain size decreases the total area of grain boundaries and the consequently decreases the scattering of electrons by these high defect concentration regions, resulting in an increase in the thermal diffusivity as suggested by Wang et al. [25].

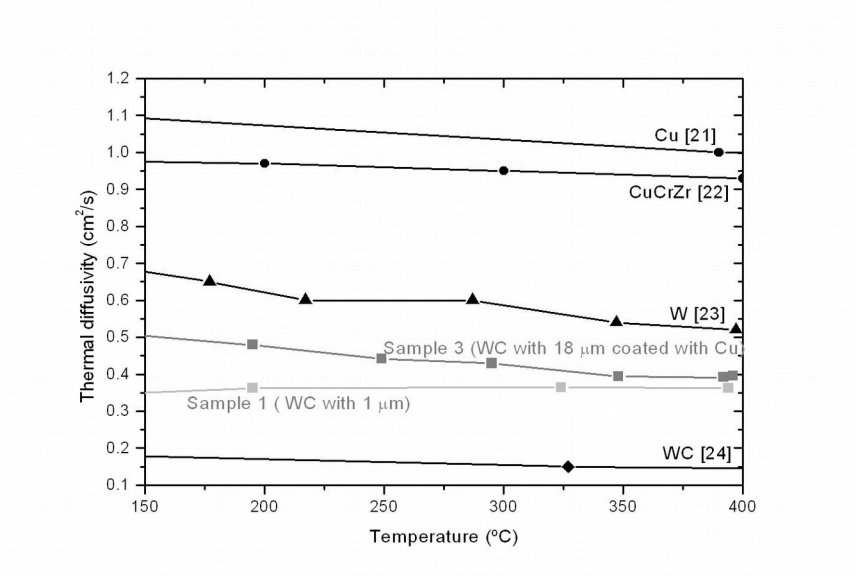

Figure 3 – Variation of thermal diffusivity of samples 1 and 3 with 50WC-50Cu composition with temperature. For comparison, the curves for pure Cu [21], CuCrZr [22], W [23] and WC [24] are also presented.

The results obtained for the measurements of Young's modulus measurements, together with those of the thermal expansion coefficient for sample 3 (50WC-50Cu composition with WC particles coated with Cu layer) are presented in Table 3. This sample exhibits a relatively low value of Young's modulus, however higher compared to pure copper [26] as was expected. Moreover, the average linear thermal coefficient assumes the value of 13.6×10^{-6} $^{o}C^{-1}$. This value is intermediate those of CuCrZr and W, which is a good indication for a thermal interlayer application. A transformation occurred between 635 ^{o}C and 850 ^{o}C, corresponding to an expansion of 1.2% of the initial length.

Table 3 – Young's modulus and thermal expansion coefficient values for the 50WC-50Cu with WC particles coated with Cu layer cermet together with the values for pure Cu and WC.

Properties	Sample 50WC-50Cu (WC coated with Cu layer)	Pure Cu	Pure WC	CuCrZr	W
Young's modulus (GPa)	200	130 [26]	600-686 [27]	128 [30]	340-405 [31]
Thermal expansion coefficient	13.6×10^{-6} $^{o}C^{-1}$	16.8×10^{-6} $^{o}C^{-1}$ [28]	5.2 -7.3$\times 10^{-6}$ $^{o}C^{1}$[29]	17×10^{-6} $^{o}C^{1}$[30]	4.5-4.6$\times 10^{-6}$ $^{o}C^{1}$ [32]

3.2 Modelling

We opted to model a monoblock with a cermet interlayer corresponding to sample 3 (50WC-50Cu composition with WC particles coated with Cu layer) as this sample had the highest densification level. The model monoblock consisted of three different layers: a W layer (plasma facing component), the interlayer under study (sample 3) and the CuCrZr tube, as shown in Figure 1. For comparison, we also modelled a monoblock with a pure copper interlayer. The simulation follows the heating of the monoblock divertor target with the 10 s, 20 MW/m^2 rectangular pulse and a subsequent cooling time of 10 s. The results, however, are shown only at the end of the heat flux pulse, as they are the most significant. Figure 4 shows the temperature distribution in the monoblock respectively with a) a pure copper interlayer and b) a cermet interlayer with contour surfaces between 250 ºC and 2250 ºC. After the pulse, the maximum temperature on the top surface of the monoblock target is higher for the case with the cermet interlayer (~2250 ºC) in comparison to pure copper (~2000 ºC). This effect is due to the lower thermal conductivity and heat capacity of the cermet interlayer which leads to a slow heat flow and consequently to a slight increase of the tungsten volume reaching temperatures above the recrystallization temperature of 1300 ºC.

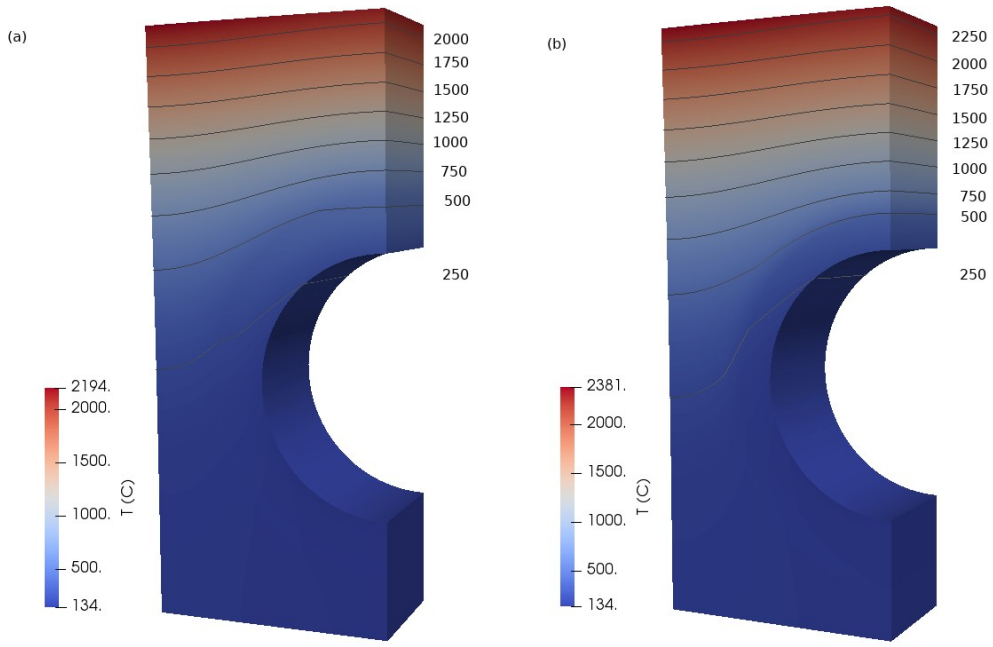

Figure 4 - Temperature distribution of the monoblock at 10 s (end of the power pulse) with (a) a copper interlayer and (b) a 50WC-50Cu cermet interlayer. Temperature contour surfaces are also shown.

The temperature on the top of the interlayer is also different in the two cases. Figure 5 shows only the interlayer and the temperature contour surfaces for (250, 350, 500 and 750 ºC) at the end of the heat flux pulse, respectively for a) pure copper and b) 50WC-50Cu cermet interlayer. The contour surfaces extend to the boundaries of the monoblock. In the first case, for copper, only a small volume exceeds 500 ºC (with a maximum temperature of 537 ºC) while for the case with 50WC-50Cu cermet interlayer a larger volume reaches temperatures between 500 and 733 ºC. In both cases, however, the temperature at the interlayer/CuCrZr interface is below the joining temperature of 580 ºC considered. Note that in both cases the top of the heat sink tube (on the inside of the interlayer) exceeds the allowed service temperature of 350 ºC.

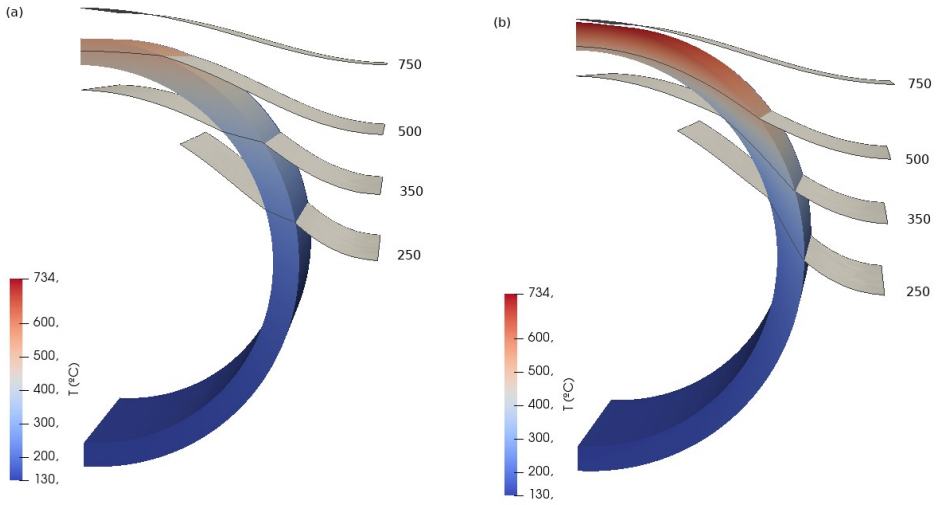

Figure 5 - Temperature distribution on the interlayer for a a) copper and a b) 50WC-50Cu interlayer. The temperature contour surfaces extend to the boundaries of the monoblock.

The effect of the interlayer material on the stress at the interface interlayer/CuCrZr tube and inside the interlayer can be estimated computing the von Mises stress values. In this case the linear elasticity model used does not consider plastic deformation and is not accurate beyond the plastic limit of each material. The computed values of the von Mises yield criterion, however, should provide a qualitative indication of the stresses in the material and allow a comparison of the behaviour of these two interlayers (pure Cu and 50WC-50Cu cermet). Figure 6 shows the von Mises values for the CuCrZr heat sink and the interlayer at the end of the heat flux pulse, respectively for the a) pure copper and b) 50WC-50Cu interlayers, together with the temperature contour surfaces.

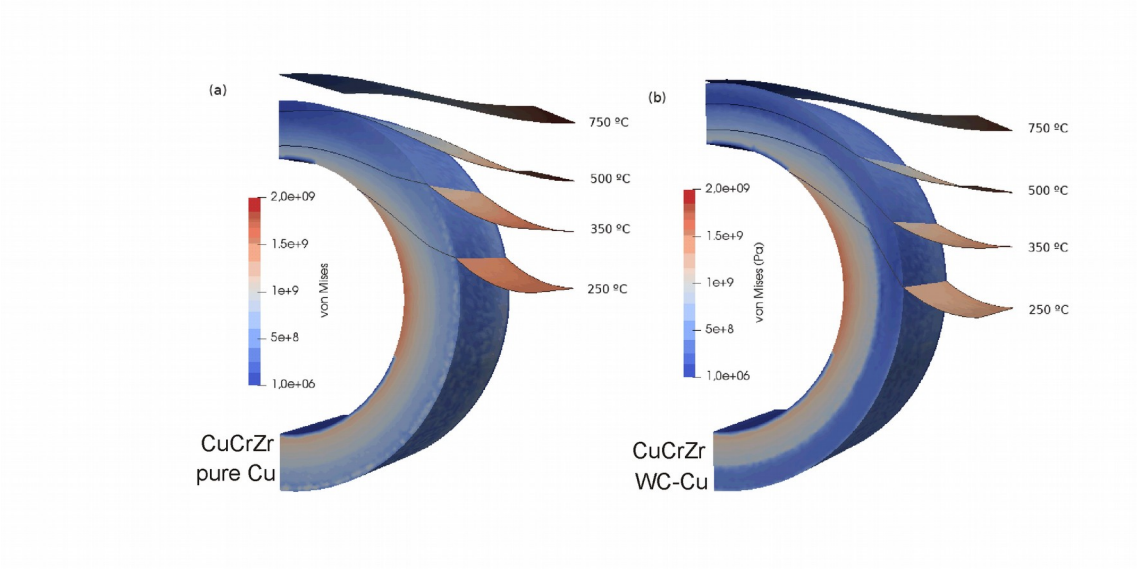

Figure 6 - Distribution of von Mises stress in the heat sink tube and interlayer at the end of the heat pulse for a) a copper and a b) 50WC-50Cu interlayer. Temperature contour surfaces as in figure 5.

In both cases the heat sink tube shows similar levels of von Mises stress, with maximum values above 1 GPa. The stress in the interlayer, however, is much smaller for the cermet than for pure copper. The effect of material type in the interlayer can be better understood plotting, in figure 7, the von Mises stress and temperature distribution along the line from the bottom to the top passing by the centre of the monoblock (indicated by the arrow in figure 1) at t=10 s. The temperature distributions is practically the same in the heat sink tube and below the cooling water tube for the two interlayer materials studied. The increase in temperature of the plasma facing surface, observed with the cermet interlayer, is established in the interlayer above the heat sink tube. The temperature variation in the tungsten is linear with height for both interlayers (pure Cu and the cermet). The inside surface of the heat sink tube shows very high values of von Mises stress which are independent of the interlayer material. In fact, this stress develops when the materials are assembled, and it is dependent on the joining temperature. The cermet interlayer presents much lower values of stress when cold and

induces also lower values of stress in the tungsten block than the pure copper interlayer. The effect of heating on the upper part of the block is actually to reduce the stress particularly in areas with temperature close to the joining temperature considered (580 ºC). The minimum value of the stress observed in the upper interlayer on the point for which, for each interlayer material, the temperature reaches the joining temperature. There is no difference in the von Mises stress values on tungsten above the heat sink tube.

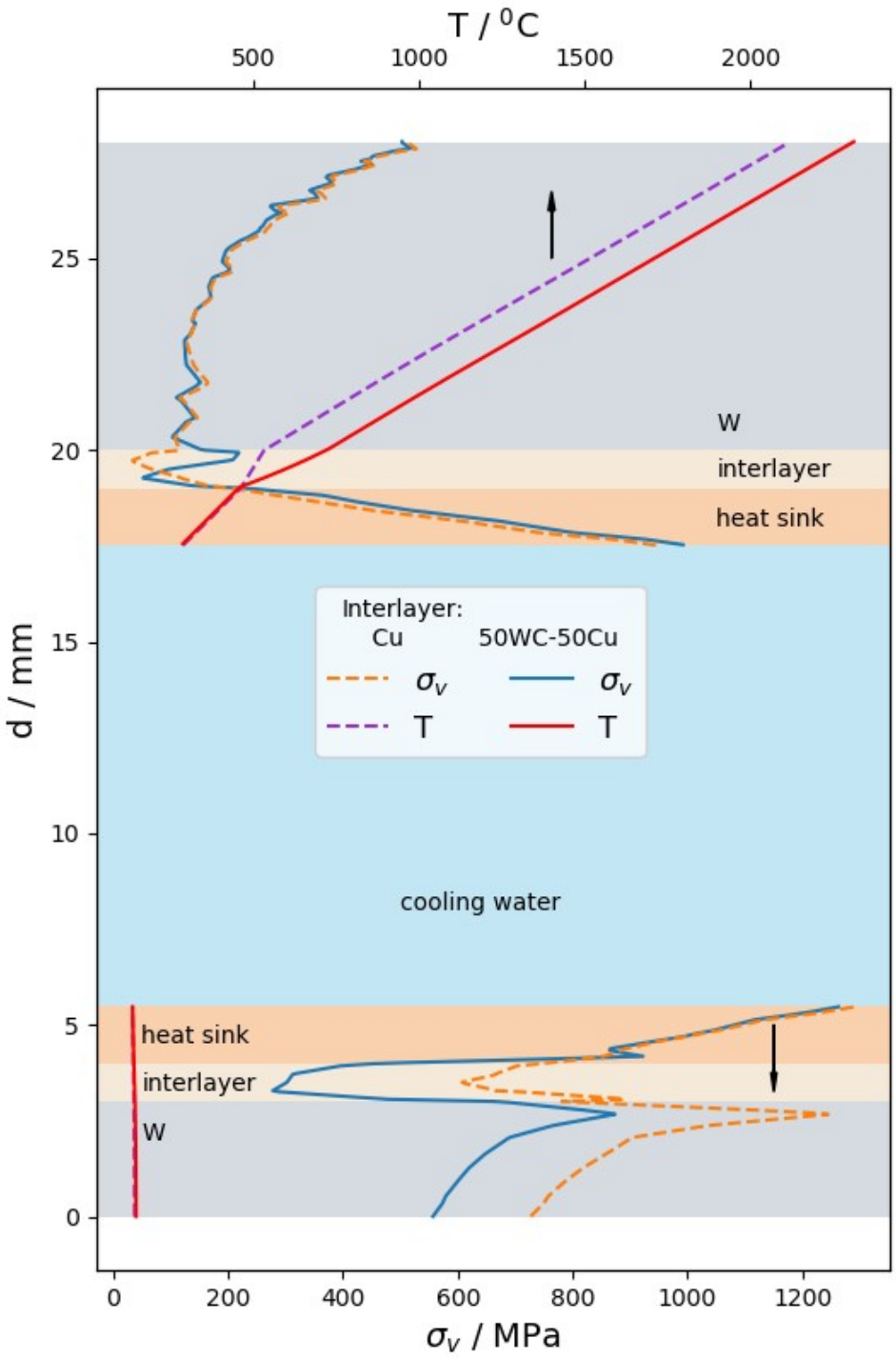

300 Figure 7 - Temperature distribution and von Mises stress along the vertical line passing through the centre of the monoblock, for the two interlayer materials studied and at the end of the heat flux pulse (10 s).

4. Conclusions

A WC-Cu composite material with 50 % volume fraction of copper was devised for thermal barriers. The samples were prepared by hot pressing at 1060 ºC with pressures of 37 MPa. The consolidated materials consisted of WC particles dispersed in the Cu matrix, without any evidence of oxide formation and with densifications between 88 and 98 %. The maximum densification value was achieved for a 50WC-50Cu sample with WC particles coated with Cu. The thermal diffusivity for the composite materials is much lower than for CuCrZr or tungsten, as desirable for thermal barrier materials. Moreover, the 50WC-50Cu sample with WC particles coated by Cu exhibits a low value of Young's modulus, however, it is higher compared to pure copper. The average linear thermal expansion coefficient was 13.6×10^{-6} $^{o}C^{-1}$ between 100 and 550 ºC. The modelling results allows predicting that the use of a WC-Cu composite instead of copper in the interlayer will lead to an increase in temperature of the upper part of the monoblock. In addition, a heat flux pulse can increase the temperature of the plasma facing surface up to 2380 ºC and lead to an increase of the tungsten recrystallized layer. The advantage of the composite interlayer lies in the significant reduction of the cold-state stress in the interlayer and tungsten.

330

Acknowledgments

This work has been carried out within the framework of the EUROfusion Consortium and has received funding from the Euratom research and training programme 2014-2018 under grant agreement No 633053. The views and opinions
335 expressed herein do not necessarily reflect those of the European Commission. Financial support was also received from the Portuguese Science and Technology Foundation (FCT) under the PTDC/CTM/100163/2008 grant, and the UID/FIS/50010/2013 and the PEST-OE/CTM-UI0084/2011 contracts. Rui M.S. Martins gratefully acknowledges FCT/MCTES for his contract under IF2014 Programme
340 (IF/00036/2014/CP1214/CT0009)". M. Dias acknowledges the FCT for the grant SFRH/BPD/68663/2010.

E. Camacho and F.M. Braz Fernandes acknowledge the funding by National Funds through the Portuguese Foundation for Science and Technology, Reference UID/ CTM/50025/2013, and FEDER funds through the COMPETE 2020 Programme under
345 project POCI-01-0145-FEDER-007688.

350

1. References

[1] S. J. Zinkle, *Phys. Scr.* T167 (2016) 14004.

[2] G. Pintsuk, et al. *Fusion Eng. Des.* 66–68 (2003) 237–240.

[3] R. Barrett *et al.*, *Fusion Eng. Des.*, 98–99 (2015) 1216–1220.

[4] J. H. You *et al.*, *Nucl. Mater. Energy* 0 (2015) 1–6.

[5] W. Shen et. al., J. Nucl. Mater. 367–370 (2007) 1449–1452.

[6] Z. Zhou et al. J. Nucl. Mater. 363–365 (2007) 1309–1314

[7] J. Song et al., J. Nucl. Mater. 442 (2013) S208–S213

[8] J.H. You et. al., J. Nucl. Mater. 438 (2013) 1–6.

[9] M. Schöbel et al., Adv. Eng. Mat., 13 (8) (2011) 742–746.

[10] M. Schöbel et al., J. Nucl. Mater. 409 (3) (2011), 225-234.

[11] R.C. Gassmann, Mater. Sci. Tech., 12 (1996), 691–696.

[12] http://www.wesltd.com/divisions/hardmetal/html/Tungsten-carbide.html

[13] M. Akoshima et al. ECTP2014 - 20th European Conference on Thermophysical Properties (2014).

[14] F. Crescenzia et al., *Fusion Eng. Des* (in press) (2018). https://doi.org/10.1016/j.fusengdes.2018.03.023

[15] Structural Design Criteria For ITER In-Vessel Components (SDC-IC), Appendix A Materials Design Limit Data, 2011.

[16] C. Geuzaine and J. Remacle, *Int. J. Numer. Meth. Engng*. 79 (2009) 1309-1331.

[17] Elmer - multiphysical simulation software, CSC - IT Center for Science (CSC), Finland; M. Malinen, P. Raback, “Elmer Finite Element Solver for Multiphysics and Multiscale Problems” in “Multiscale Modelling Methods for Applications in Materials Science”, edited by I. Kondov, G. Sutmann 2013.

[18] M. Li, J-H. You, *Nucl. Mat. Energy* 14 (2018) 1-7

[19] J.M. Molina, et al., *Curr. Opin. Solid State Mater. Sci.* 9 (2005) 202–210.

[20] M. Dias et al. *Fus. Eng. Des.* (submited)

[21]https://www.netzsch-thermal-analysis.com/en/materials-applications/thermoelectric/pure-copper-thermal-diffusivity/

[22] M. Rohde et al., High Temperatures-High Pressures, Old City Publishing, Inc. (2013)

[23] M. Futjitsuka et al. *J. Nucl. Mater.* 238-287 (2000) 1148-1151.

[24] M. Akoshima et al. ECTP2014 - 20th European Conference on Thermophysical Properties (2014).

[25] Wang, International Journal of Refractory Metals and Hard Materials 49 (2014) 170-177.

[26] L.B. Freund, S. Suresh. Thin Film Materials: Stress, Defect Formation, and Surface Evolution (2003)

[27] https://www.azom.com/properties.aspx?ArticleID=1203

[28] https://www.engineeringtoolbox.com/thermal-expansion-metals-d_859.html

[29] P. Hidnert, Part of Journal of Research of the National Bureau of Standards, (18) (1937)

[30] http://www.conductivity-app.org/alloy-sheet/19

[31] https://www.azom.com/properties.aspx?ArticleID=614

[32]ASM Ready Reference, Thermal properties of metals, ASm materials Data Series, Fran Cverna, technical Editor.